

Superacidic or Not...? Synthesis, Characterisation, and Acidity of the Room-Temperature Ionic Liquid $[C(CH_3)_3]^+[Al_2Br_7]^-$ Franziska Scholz, Daniel Himmel, Harald Scherer, and Ingo Krossing*^[a]

Abstract: The room-temperature ionic liquid (RT-IL) $[C(CH_3)_3]^+[Al_2Br_7]^-$ (m.p. 2 °C) was generated by bromide abstraction from *tert*-butyl bromide with the Lewis acid aluminum bromide in the absence of solvent. The crystal structure of the *tert*-butyl cation salt was determined by X-ray diffraction. NMR, IR, and Raman spectroscopy, as well as quantum-chemical and thermo-

dynamic calculations, confirm the composition of this RT-IL. Thus, one may consider this RT-IL to be a readily accessible (and on a large scale) cationic Brønsted acid (protonated isobutene)

with the potential for further reactivity. Based on the new absolute Brønsted acidity scale, we calculated an absolute pH_{abs} value of 171 for liquid bulk $[C(CH_3)_3]^+[Al_2Br_7]^-$. This value is about as acidic as 100% sulfuric acid ($pH_{abs} = 171$) and, thus, on the edge of superacidity.

Keywords: carbocations • ionic liquids • Lewis acids • superacidic systems • X-ray diffraction

Introduction

Alkyl cations have been the subject of many investigations^[1–4] and they are key intermediates in many organic reactions. In magic acid, $HfSO_3/SbF_5$, Olah et al.^[3,5] characterised tertiary alkyl cations at low temperatures by NMR spectroscopy. However, attempts to confirm their structure in the single-crystalline state were problematic. The first structural characterisation of the *tert*-butyl cation was achieved in 1993 in the form of its $[Sb_2F_{11}]^-$ salt.^[6] Buzek et al.^[7] confirmed these results by using ab initio calculations. Reed and co-workers^[8–10] reported the isolation of the $[C(CH_3)_3]^+$ ion and other simple tertiary alkyl cations at room temperature by using their substituted carborane anions as counterions. Despite the very high stability of the latter salts, their straightforward synthesis on a larger scale is restricted because the starting material, $CH_3[HCB_{11}Me_5X_6]$ ($X = Cl, Br$), is only available on a milligram scale. Herein, we were interested in whether a stable $[C(CH_3)_3]^+$ salt was accessible with a more straightforwardly accessible counterion.

For the stabilisation of carbocations, the counterions need to be rather stable, non-nucleophilic, and non-basic. The sta-

bility of halometallate anions is usually coupled to the acidity of the underlying Lewis acid. As a quantitative scale of acidity, fluoride-ion affinities (FIA), which hark back to the pioneering work of Bartlett and co-workers,^[11] are often used. Applied to the given system, the FIA of monomeric aluminum bromide (494 kJ mol^{-1}) is a bit higher than that of monomeric SbF_5 (489 kJ mol^{-1}).^[12] Hence, monomeric gaseous aluminium bromide is a Lewis superacid, which is defined as a molecular Lewis acid that is stronger than gaseous monomeric SbF_5 ,^[12,13] and it is more suitable and easier-to-handle for such transformations than SbF_5 itself. In agreement with this result, solutions of $AlBr_3$ in CH_2Br_2/CH_2Cl_2 are known to stabilize tertiary alkyl cations at temperatures of about -30°C and the in situ solution-state stabilisation of the *tert*-butyl cation in $AlBr_3$ with liquid HBr as a solvent at -25°C has already been shown by NMR spectroscopy. No isolation of the latter compound and related compounds has hitherto been reported.^[14–17] In the system $AlBr_3/Br^-$, until now, two counterions have been structurally characterised: $[AlBr_4]^-$ and $[Al_2Br_7]^-$. The existence of $[Al_3Br_{10}]^-$ in molten $(KBr)_y(AlBr_3)_{1-y}$, with $y = 0.25–0.33$, has also been suggested based on neutron-diffraction data.^[18]

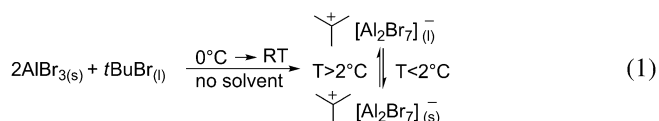
Herein, the properties of $AlBr_3$ (in contrast to the non-oxidising magic acid) and the low nucleophilicity of the $[Al_2Br_7]^-$ ion were found to be capable of stabilising the *tert*-butyl cation at room temperature. The title compound, $[C(CH_3)_3]^+[Al_2Br_7]^-$, exhibits a melting point of 2°C and, thus, can be classified as a room-temperature ionic liquid.^[19] We also evaluate the bulk acidity of this compound with respect to the recently introduced absolute Brønsted acidity scale.^[20,21]

[a] Dipl. Chem. F. Scholz, Dr. D. Himmel, Dr. H. Scherer, Prof. Dr. I. Krossing
Institut für Anorganische und Analytische Chemie
Freiburger Materialforschungszentrum (FMF) and
Freiburg Institute for Advanced Studies (FRIAS)
Universität Freiburg
Albertstrasse 19, 79104 Freiburg (Germany)
E-mail: krossing@uni-freiburg.de

Supporting information for this article, including a detailed description of the quantum-chemical calculations, experimental procedures, a full list of the calculated and experimental vibrational frequencies, and crystallographic tables, is available on the WWW under <http://dx.doi.org/10.1002/chem.201203260>.

Results and Discussion

Synthesis of $[\text{C}(\text{CH}_3)_3]^+[\text{Al}_2\text{Br}_7]^-$: Our first attempts at the preparation of $[\text{C}(\text{CH}_3)_3]^+[\text{Al}_2\text{Br}_7]^-$ showed that the synthesis of the *tert*-butyl cation from *t*BuBr and AlBr_3 in solvent was always accompanied by side reactions: In CH_2Cl_2 , halide exchange took place and the formation of AlCl_3 was observed; In CH_2Br_2 , the reactants indeed dissolved as reported.^[14] However, in our hands, the existence of the *tert*-butyl cation could not be verified by NMR spectroscopy. Fluorinated aromatic solvents, such as *ortho*-difluorobenzene, immediately underwent alkylation. Finally, the reactions between *tert*-butyl bromide and AlBr_3 were carried out without solvent ([Eq. (1)]).



Upon reaction for 15 min at 0°C and subsequent warming to room temperature, a highly viscous, air- and moisture-sensitive liquid formed. Under an inert atmosphere, this solution turned out to be remarkably stable at room temperature (by NMR spectroscopy). At 2°C , the oil reversibly crystallised, thus characterising this compound as a RT-IL (Figure 1).

At 0°C , the crystalline product can be stored for months without decomposition. In a closed flask or an NMR tube, slow partial decomposition occurs at room temperature, accompanied by the formation of (mainly) protonated isobutene oligomers, until an equilibrium HBr pressure is reached. This decomposition can be prevented, to a large extent, by adding additional HBr pressure. Thus, a sealed NMR sample of $[\text{C}(\text{CH}_3)_3]^+[\text{Al}_2\text{Br}_7]^-$ with a pressure of

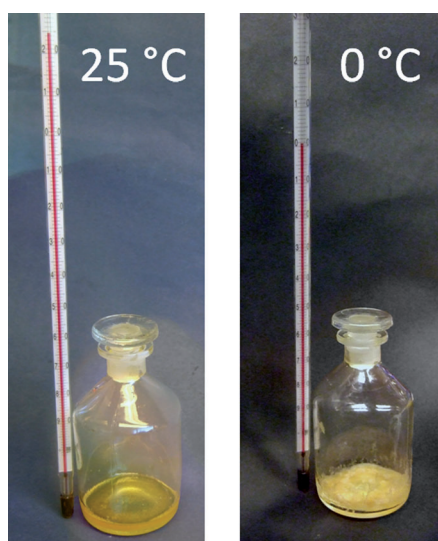


Figure 1. Left: Liquid $[\text{C}(\text{CH}_3)_3]^+[\text{Al}_2\text{Br}_7]^-$ at room temperature. Right: Solid $[\text{C}(\text{CH}_3)_3]^+[\text{Al}_2\text{Br}_7]^-$ at 0°C .

HBr of about 0.3 bar remained unchanged for one year at room temperature.

NMR spectroscopic characterisation of $[\text{C}(\text{CH}_3)_3]^+[\text{Al}_2\text{Br}_7]^-$: With our optimised procedure in hand and under additional HBr pressure, as-prepared $[\text{C}(\text{CH}_3)_3]^+[\text{Al}_2\text{Br}_7]^-$ was characterised by ^1H , ^{13}C , and ^{27}Al NMR spectroscopy at room temperature. The presence of the *tert*-butyl cation was confirmed by characteristic shifts at ^1H NMR: $\delta = 2.6$ ppm, ^{13}C NMR: $\delta = 325$ (C_q) and 49 ppm (CH_3), and ^{27}Al NMR: $\delta = 82$, which were in accord with literature data.^[1,2,15,22] Some additional weak signals were also detected by NMR spectroscopy, which suggested the formation of isobutene oligomers (for the actual spectra, see the Supporting Information).

Solid-state structure of $[\text{C}(\text{CH}_3)_3]^+[\text{Al}_2\text{Br}_7]^-$ and accompanying *ab initio* structure optimisations: Figure 2 shows the asymmetric unit in the crystal structure of $[\text{C}(\text{CH}_3)_3]^+[\text{Al}_2\text{Br}_7]^-$ ($R_1 = 0.0491$, $wR_2 = 0.1111$). The structural details of the $[\text{Al}_2\text{Br}_7]^-$ ion are close to those found in $\text{K}[\text{Al}_2\text{Br}_7]$ ^[23] and $\text{NH}_4[\text{Al}_2\text{Br}_7]$.^[24] There are two independent cations in the asymmetric unit, one of which is intrinsically disordered over two positions because its central C atom is located on an inversion centre.

From the sum of the C-C⁺-C bond angles, $360.0(7)^\circ$, the ordered carbocation was judged to be planar and its average C-C distance (1.45 Å) is in good agreement with earlier structures.^[6,8] The solid-state packing of this AB salt is of a

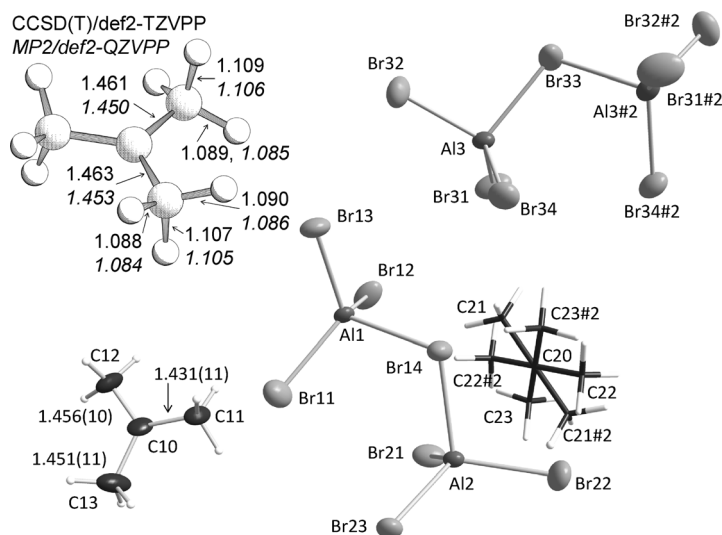


Figure 2. Molecular structure of $[\text{C}(\text{CH}_3)_3]^+[\text{Al}_2\text{Br}_7]^-$. Thermal ellipsoids are set at 50% probability (except for H atoms and the disordered cation). Selected bond lengths [Å] and angles [°]: Br11–Al1 2.222(2), Br13–Al1 2.246(2), Br12–Al1 2.252(2), Br14–Al1 2.435(2), Br14–Al2 2.406(2), Br21–Al2 2.257(2), Br22–Al2 2.264(2), Br23–Al2 2.254(2); Al1–Br14–Al2 108.03(7), Br11–Al1–Br12 114.26(9), Br11–Al1–Br13 112.89(9), Br12–Al1–Br13 114.22(9), Br21–Al2–Br22 113.03(9), Br22–Al2–Br23 113.02(9), Br21–Al2–Br23 113.79(9), C11–C10–C13 120.2(7), C12–C10–C13 120.7(7), C11–C10–C12 119.1(7). Inset (top-left): Calculated bond lengths [Å] of $[\text{C}(\text{CH}_3)_3]^+$ with C_3 symmetry (CCSD(T)/def2-TZVPP, MP2/def2-QZVPP level).

distorted CsCl type (see the Supporting Information). Anion–cation interactions were analysed by Hirshfeld surface analysis (with Crystal Explorer).^[25–28] For this analysis, all of the C–H distances were set by the program to 1.083 Å (derived from neutron-diffraction data). The Hirshfeld surface of the disordered cation includes a volume of 107.7 Å³, whereas the non-disordered cation has a slightly smaller Hirshfeld volume of 98.3 Å³. Figure 3 shows the Hirshfeld cation surface, surrounded by the eight nearest-neighbouring $[\text{Al}_2\text{Br}_7]^-$ counterions.^[29]

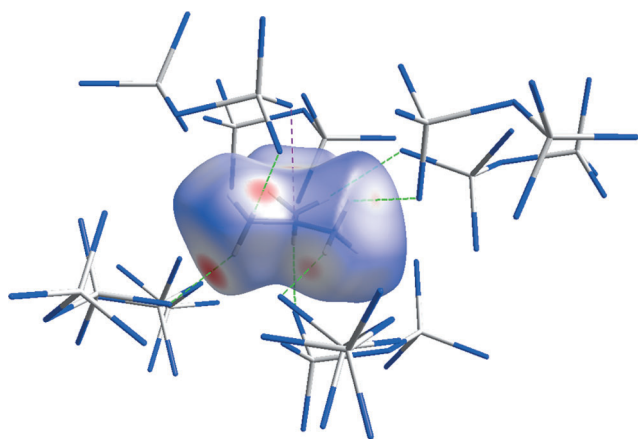


Figure 3. Hirshfeld surface of the $[\text{C}(\text{CH}_3)_3]^+$ ion with surrounding counterions. The red colour indicates contact distances that are shorter than the sum of the van der Waals radii; the blue colour indicates contact distances that are longer than the sum of the van der Waals radii.

Accompanying ab initio structure optimisations were performed at the MP2 and CCSD(T) levels of theory with the def2-TZVPP^[30] basis sets, as well as def2-QZVPP in the case of MP2. At the MP2 level, the maximum deviation between the triple- ζ - and quadruple- ζ -calculated bond lengths was 0.002 Å, which indicates almost-converged structures with the smaller def2-TZVPP basis set. Both methods yielded C_s structures that agreed to within 0.011 Å, with no imaginary frequencies for the MP2/def2-QZVPP structure (no frequencies for CCSD(T)). At both levels, one C–H bond in every methyl group is clearly elongated by 0.02 Å compared to the other two, owing to hyperconjugation with the empty p orbital on the central C atom. This result is in agreement with the IR spectra, in which the main C–H stretch of the cation appears red-shifted at 2787 cm⁻¹, when compared to the C–H stretches of free isobutene (2893–3086 cm⁻¹).^[31] Similar calculations at the ccSD(t)/cc-pVXZ (X=T, Q) level were published very recently, with almost identical results.^[32]

Vibrational spectroscopy: The IR and Raman measurements show the expected bands and are in good agreement with the calculated (PBE0/def2-TZVPP; Figure 4) and experimental spectra of $[\text{C}(\text{CH}_3)_3]^+[\text{Sb}_2\text{F}_{11}]^-$ ^[33] (Table 1). The main C–H stretch of the cation appears at 2787 cm⁻¹. Interestingly, this stretching frequency is in-between the values found

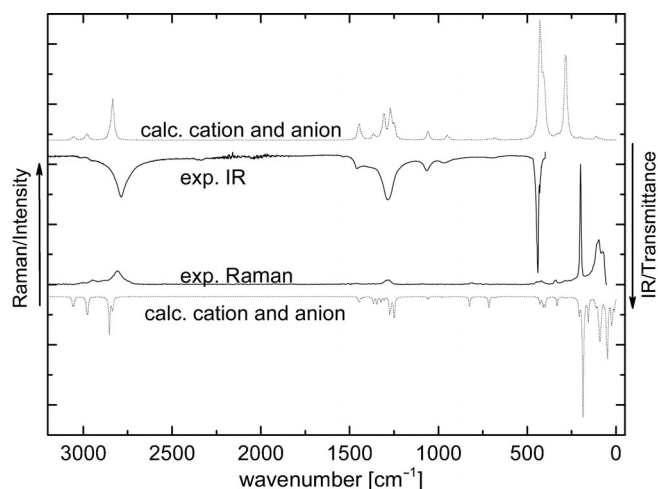
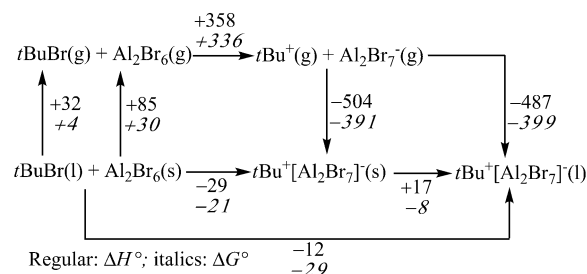


Figure 4. Experimental and calculated (scaling factor: 0.96, PBE0/def2-TZVPP) IR and Raman spectra of $[\text{C}(\text{CH}_3)_3]^+[\text{Al}_2\text{Br}_7]^-$.

in $[\text{C}(\text{CH}_3)_3]^+[\text{HCB}_{11}\text{Me}_5\text{Br}_6]^-$ (2695 cm⁻¹)^[8] and $[\text{C}(\text{CH}_3)_3]^+[\text{Sb}_2\text{F}_{11}]^-$ (2830 cm⁻¹),^[4] thus suggesting that the basicity of the $[\text{Al}_2\text{Br}_7]^-$ ion also lies in-between these two anions.

Formation and phase-change thermodynamics: To investigate the overall reaction thermodynamics that lead to solid or liquid $[\text{C}(\text{CH}_3)_3]^+[\text{Al}_2\text{Br}_7]^-$, we constructed a Born–Fajans–Haber cycle (BFHC) by combining experimental data, semi-empirical correlations, and highly correlated quantum-chemical calculations up to the CCSD(T)-level (for a detailed description, see Scheme 1 and the Supporting



Scheme 1. Born–Fajans–Haber cycle to assess the reaction enthalpy and Gibbs reaction energy [kJ mol⁻¹]. Values in italics are standard Gibbs energies; those in regular font are standard enthalpies at 298 K, 1 bar.

Information). Lattice Gibbs energies/enthalpies were calculated according to a recently published approach that was optimised for ionic liquids.^[34,35] The condensed-phase thermodynamics that were established with this cycle were in very good agreement with the experimental observations: The reaction of liquid *tert*-butyl bromide with solid AlBr_3 was calculated to be slightly exothermic and exergonic for the formation of solid—as well as liquid— $[\text{C}(\text{CH}_3)_3]^+[\text{Al}_2\text{Br}_7]^-$. In both cases, the main driving force for the reaction is the gain in lattice/solvation energy in the condensed solid/liquid phase from the gaseous ions. The gas-

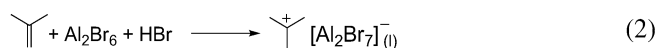
Table 1. IR and Raman bands of liquid $[\text{C}(\text{CH}_3)_3]^+[\text{Al}_2\text{Br}_7]^-$, PBE0/def2-TZVPP-calculated scaled (0.96) harmonic frequencies of superposed $[\text{C}(\text{CH}_3)_3]^+$ and $[\text{Al}_2\text{Br}_7]^-$ bands, and comparison with known $[\text{C}(\text{CH}_3)_3]^+$ and $[\text{Al}_2\text{Br}_7]^-$ salts.^[a]

$[\text{C}(\text{CH}_3)_3]^+[\text{Al}_2\text{Br}_7]^-$		$[\text{C}(\text{CH}_3)_3]^+[\text{Sb}_2\text{F}_{11}]^-$		Assignment
Calculated	Raman Experimental	Calculated	IR	
3060 (0.16)	2995 (0.02)	3056 (0.56)	3018 (0.05)	$\nu_a \text{CH}_3$
3054 (0.16)				
2978 (0.10)	2950 (0.04)	2978 (0.57)	2953 (0.07)	$\nu_a \text{CH}_3$
2853 (0.20)	2809 (0.12)	2834 (0.70)	2787 (0.37)	$\nu_s \text{CH}_3$
2837 (0.38)				
		1498 (0.03)	1533 (0.04)	$\delta_{\text{bend}} \text{CH}_3$
1444 (0.13)	1488 (0.01)			$\delta_{\text{bend}} \text{CH}_3$
		1447 (0.61)	1458 (0.14)	$\delta_{\text{bend}} \text{CH}_3$
1430 (0.10)	1463 (0.01)			$\delta_{\text{bend}} \text{CH}_3$
1366 (0.15)	1396 (0.01)			$\delta_{\text{bend}} \text{CH}_3$
1347 (0.15)	1366 (0.01)	1368 (0.57)		$\delta_{\text{bend}} \text{CH}_3$
1324 (0.13)	1295 (0.04)			$\delta_{\text{bend}} \text{CH}_3$
1307 (0.12)	1281 (0.04)	1303 (0.65)	1283 (0.40)	$\delta_{\text{bend}} \text{CH}_3$
1275 (0.23)	1241 (0.01)	1271 (0.67)		$\delta_{\text{bend}} \text{CH}_3$
1250 (0.25)	1220 (0.01)	1251 (0.61)		$\delta_{\text{bend}} \text{CH}_3$
1059 (0.11)	1089 (0.01)	1062 (0.58)	1065 (0.15)	$\delta_{\text{bend}} \text{CH}_3/\nu_a \text{CC}$
978 (0.10)	992 (0.01)			$\delta_{\text{rock}} \text{CH}_3/\nu_s \text{CC}$
		951 (0.57)	968 (0.09)	$\delta_{\text{rock}} \text{CH}_3/\nu_a \text{CC}$
951 (0.09)	950 (0.01)			$\delta_{\text{rock}} \text{CH}_3/\nu_a \text{CC}$
942 (0.09)				$\delta_{\text{rock}} \text{CH}_3/\nu_a \text{CC}$
825 (0.16)	815 (0.02)	821 (0.55)		$\nu_s \text{CC}$
	765 (0.01)			$\nu_s \text{CC}$
716 (0.17)	732 (0.01)	717 (0.55)		$\nu_s \text{CCC}/\delta_{\text{bend}} \text{CH}_3$
682 (0.10)		684 (0.56)	696 (0.05)	$\delta_{\text{rock}} \text{CH}_3$
		430 (1.0)	440 (1.0)	$\nu_{\text{a,t}} \text{Al-Br}$
428 (0.15)	420 (0.03)			$\nu_{\text{a,t}} \text{Al-Br}$
411 (0.17)		410 (0.81)		$\delta_s \text{C-C}/\delta_{\text{bend}} \text{CH}_3$
401 (0.17)				$\nu_{\text{a,t}} \text{Al-Br}$
332 (0.16)	341 (0.04)	332 (0.57)		$\nu_{\text{a,b}}, \nu_{\text{s,t}}, \delta_s \text{Al-Br}$
		287 (0.87)		$\delta_a \text{CC}$
284 (0.10)	283 (0.03)	280 (0.86)	286 (vw)	$\nu_{\text{a,b}}, \nu_{\text{s,t}}, \delta_s \text{Al-Br}$
207 (0.24)			201 (vs)	$\nu_{\text{s,t}}, \nu_{\text{a,b}}, \delta_s \text{Al-Br}$
186 (1.0)	202 (1.0)	202 (0.56)		$\nu_{\text{s,t}}, \nu_{\text{a,b}}, \delta_s \text{Al-Br}$
156 (0.29)		156 (0.55)	125 (m)	$\nu_{\text{s,t}}, \delta_s \text{Al-Br}$
112 (0.18)		111 (0.56)	114 (m)	$\delta_s \text{Al-Br}$
90 (0.43)	99 (0.37)		99 (m)	$\delta_s \text{Al-Br}$
48 (0.28)	78 (0.27)			$\delta_s \text{Al-Br}$

[a] Frequencies are given in cm^{-1} , intensities in parentheses are normalised to 1.0; italic font indicates the frequencies of the $[\text{Al}_2\text{Br}_7]^-$ ion, regular font indicates the frequencies of the $[\text{C}(\text{CH}_3)_3]^+$ ion. ν : stretching mode, δ : deformation mode, rock: rocking mode, bend: bending mode, a: antisymmetric mode, s: symmetric mode, b: bridged mode, t: terminal mode.

phase reaction is energetically highly disfavoured, owing to charge separation. The calculated enthalpy of fusion of $[\text{C}(\text{CH}_3)_3]^+[\text{Al}_2\text{Br}_7]^-$ ($+17 \text{ kJ mol}^{-1}$) is typical for ILs ($15\text{--}25 \text{ kJ mol}^{-1}$),^[34] whilst the slightly negative Gibbs energy of fusion (-8 kJ mol^{-1}) corresponds to a melting point that is somewhat below room temperature.

Investigation of the (super-?)acidity and absolute acidity of $[\text{C}(\text{CH}_3)_3]^+[\text{Al}_2\text{Br}_7]^-$: Farcasiu et al.^[36] and Kramer^[37] have previously suggested that the mixture of HBr and AlBr_3 is one of the strongest superacids known, although this statement has been disputed.^[33] The acidic properties of HBr/ 2AlBr_3 are apparently strong enough to shift the equilibrium in Equation (2) almost completely to the right-hand side.



In agreement with Equation (2), we observed that a sample of $[\text{C}(\text{CH}_3)_3]^+[\text{Al}_2\text{Br}_7]^-$ in a sealed NMR tube with 0.3 bar HBr pressure remained unchanged for one year at room temperature. Separate experiments (see the Supporting Information) showed that the reaction of AlBr_3 with 0.5 equivalents of isobutene under an atmosphere of HBr (1.6 equiv) gave a mixture of hydrocarbons and higher-mass carbocations. No terminal-alkene moieties were observed by NMR spectroscopy. This result implies that the formation of $[\text{C}(\text{CH}_3)_3]^+[\text{Al}_2\text{Br}_7]^-$ from isobutene and HBr/ AlBr_3 is accompanied by polymerisation and yields a mixture of com-

pounds that appear to be kinetically stable under these conditions. In the absence of extra HBr pressure, the formation of higher-mass carbocations from pure [C(CH₃)₃]⁺[Al₂Br₇]⁻ was evident. This formation could largely be prevented through the law of mass action by the application of slight HBr pressure (see above).

Based on these above-summarised observations, we will now analyse the reactions that are responsible for the Brønsted acidity of [C(CH₃)₃]⁺[Al₂Br₇]⁻ in bulk medium. In contrast to molecular liquids, this “autoprotolysis reaction” of the pure [C(CH₃)₃]⁺[Al₂Br₇]⁻ liquid is somewhat more complicated. Our main assumptions are: 1) That the *tert*-butyl cation acts as a Brønsted acid ([Eq. (3)]).

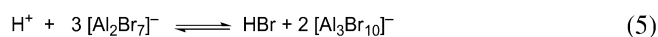


2) That the formed isobutene undergoes cationic polymerisation ([Eq. (4)]).



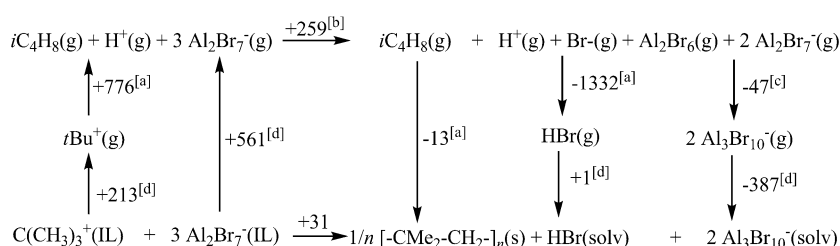
On the way to the neutral polyisobutene, the observed higher-mass carbocations that result from the addition of isobutene to the *tert*-butyl cation are the natural intermediates.

3) That the solvated proton decomposes the [Al₂Br₇]⁻ anion, with the formation of HBr and [Al₃Br₁₀]⁻ ([Eq. (5)]).



Therefore, the overall decomposition reaction should be the sum of Equations (3)–(5). We constructed a BFHC (Scheme 2) that analysed the decomposition of [C(CH₃)₃]⁺[Al₂Br₇]⁻. By combining the available experimental values, high-level quantum-chemical calculations, and COSMO-RS^[38,39] to calculate the Gibbs solvation energies, the underlying energetics could be assessed.

As a standard state for the IL-forming [C(CH₃)₃]⁺ and [Al₂Br₇]⁻ ions, we used the pure liquid [C(CH₃)₃]⁺[Al₂Br₇]⁻ IL in the COSMO-RS calculations (denoted as (IL) in Scheme 2) so that their activities were set to 1 and could be removed from the decomposition equilibrium. For solid polyisobutene, the activity could also be set to 1. For the description of the [Al₃Br₁₀]⁻ ion and HBr, we used an ideal



Scheme 2. Born–Fajans–Haber cycle to assess the Gibbs energy of decomposition at 298 K, 1 bar. a) Experimental value;^[40] b) value calculated by using a ccSD(T)/MP2 compound method (for details, see the Supporting Information); c) calculated MP2/(Al: aug-cc-pV(T+d)Z, Br: aug-cc-pVTZ-PP) reaction energy with thermal/entropic corrections at the BP86/def-TZVP level; d) value calculated by using the COSMO-RS model.^[38,39]

1 M solution in the IL as the standard state (denoted as (solv)). By using these conventions, the law of mass action for this autoprotolysis is given by Equation (6).

$$K_{\text{AP}} = a(\text{HBr}(\text{solv})) \times a(\text{Al}_3\text{Br}_{10}^-(\text{solv}))^2 \\ = \exp\left(-\frac{31 \text{ kJ mol}^{-1}}{R \times 298.15 \text{ K}}\right) = 3.7 \times 10^{-6} \quad (6)$$

With $a(\text{Al}_3\text{Br}_{10}^-(\text{solv})) = 2a(\text{HBr}(\text{solv}))$, one obtains Equation (7).

$$a(\text{HBr}(\text{solv})) = \sqrt[3]{K_{\text{AP}}/4} = 9.8 \times 10^{-3} \text{ and} \\ a(\text{Al}_3\text{Br}_{10}^-(\text{solv})) = 1.95 \times 10^{-2} \quad (7)$$

In terms of our recently introduced absolute Brønsted acidity scale,^[20,21] the absolute chemical potential of the proton, $\mu_{\text{abs}}(\text{H}^+)$, was defined as the lowering of its chemical potential compared to its standard state in the gas phase. $\mu_{\text{abs}}(\text{H}^+)$ corresponds to the pressure of a (hypothetical) ideal gas of protons and to an “absolute pH value” pH_{abs} (note that $RT \ln 10 = 5.71 \text{ kJ mol}^{-1}$ at 298.15 K), according to Equation (8) and (9).

$$\mu_{\text{abs}}(\text{H}^+) = RT \ln\left(\frac{p(\text{H}^+, \text{ideal})}{1 \text{ bar}}\right) = -5.71 \text{ kJ mol}^{-1} \times \text{pH}_{\text{abs}} \quad (8)$$

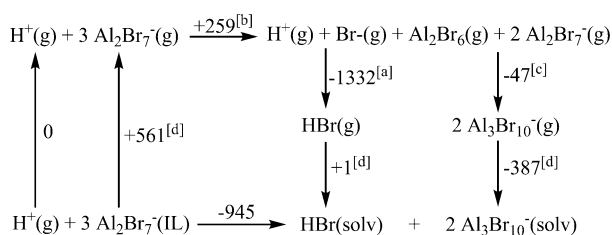
with

$$\text{pH}_{\text{abs}} = -\log\left(\frac{p(\text{H}^+, \text{ideal})}{1 \text{ bar}}\right) \quad (9)$$

In a solvent (S) at room temperature, the chemical potential of the proton follows Equation (10).

$$\mu_{\text{abs}}(\text{H}^+) = \mu_{\text{abs}}^\circ(\text{H}^+, \text{S}) + RT \ln a(\text{H}^+, \text{S}) \\ = \Delta_{\text{solv}} G^\circ(\text{H}^+, \text{S}) - 5.71 \text{ kJ mol}^{-1} \times \text{pH} \text{ with } \mu_{\text{abs}}^\circ(\text{H}^+, \text{S}) \\ = \Delta_{\text{solv}} G^\circ(\text{H}^+, \text{S}) \quad (10)$$

To calculate the absolute chemical potential of the proton in the [C(CH₃)₃]⁺[Al₂Br₇]⁻ IL, we constructed a BFHC (Scheme 3) to establish the standard Gibbs solvation energy of the proton in the pure IL. As a basis for this assessment, we suggest that the solvation of the proton in the IL only proceeds by interactions with the only base that is present,



Scheme 3. Born–Fajans–Haber cycle to assess the standard Gibbs energy of solvation in $[\text{C}(\text{CH}_3)_3]^+[\text{Al}_2\text{Br}_7]^-$ at 298 K, 1 bar: a) Experimental value;^[40] b) value calculated by using a ccscd(t)/MP2 compound method (for details, see the Supporting Information); c) calculated MP2/(Al: aug-cc-pV(T+d)Z, Br: aug-cc-pVTZ-PP) reaction energy with thermal/entropic corrections at the BP86/def-TZVP level; d) value calculated by using the COSMO-RS model.^[38,39] For full details, see the Supporting Information.

that is, the $[\text{Al}_2\text{Br}_7]^-$ ion in the IL.

To place this value in context, the calculated standard Gibbs solvation energy of the proton in the $[\text{C}(\text{CH}_3)_3]^+[\text{Al}_2\text{Br}_7]^-$ IL, -945 kJ mol^{-1} , is in between the standard values for fluorosulfonic acid (-924 kJ mol^{-1}) and sulfuric acid (-966 kJ mol^{-1}).^[21] The solvation constant of the proton is calculated by Equation (11) or, in logarithmic form, by Equation (12).

$$K_{\text{solv}}(\text{H}^+, \text{IL}) = \frac{a(\text{HBr}(\text{solv})) \times a(\text{Al}_3\text{Br}_{10}^-(\text{solv}))^2}{p(\text{H}^+(\text{g})) \times 1 \text{bar}^{-1}} \quad (11)$$

$$= \exp\left(\frac{945 \text{ kJ mol}^{-1}}{R \times 298.15 \text{ K}}\right) = 3.1 \times 10^{165}$$

$$165.5 = \log K_{\text{solv}} = \frac{\Delta_{\text{solv}}G^\circ(\text{H}^+, \text{IL})}{RT \ln 10} = \log a(\text{HBr}(\text{solv})) \quad (12)$$

$$+ 2 \log a(\text{Al}_3\text{Br}_{10}^-(\text{solv})) + \text{pH}_{\text{abs}}$$

Using the calculated equilibrium activities of the solvated HBr and $[\text{Al}_3\text{Br}_{10}]^-$ particles, the absolute acidity in the liquid $[\text{C}(\text{CH}_3)_3]^+[\text{Al}_2\text{Br}_7]^-$ IL at room temperature was calculated according to Equation (13).

$$\text{pH}_{\text{abs}} = 165.5 - \log(9.8 \times 10^{-3}) - 2 \times \log(1.95 \times 10^{-2}) \quad (13)$$

$$= 170.9 \text{ or } \mu_{\text{abs}}(\text{H}^+) = -976 \text{ kJ mol}^{-1}$$

A practically identical absolute acidity of pure sulfuric acid, with $\text{pH}_{\text{abs}} = 170.8$ or $\text{pH}_{\text{abs}}(\text{H}^+) = -975 \text{ kJ mol}^{-1}$, was recently established. Assuming an error bar of 15–20 kJ mol^{-1} for both calculations, we conclude that the thermodynamic acidity of liquid $[\text{C}(\text{CH}_3)_3]^+[\text{Al}_2\text{Br}_7]^-$ is about the same as that of neutral anhydrous sulfuric acid.

Bracketing the stability of the *t*Bu⁺ cation in molecular acids:

By using a ladder of indicator bases, Hammett and Deyrup^[41] introduced the Hammett acidity function (H_0) for the quantification of acid strength in non-aqueous media. The *t*Bu cation is known to be unstable in neat sulfuric acid, which has an experimentally determined H_0 value of -12.0 . Reed and co-workers reported^[9] that the *t*Bu cation is only

stable when the H_0 value is smaller than -17 . However, Olah et al. stated that “when solutions of alcohols in fluoro-sulfonic acid or fluorosulfonic acid/sulfur dioxide were prepared, tertiary carbonium ions could be generally observed, but peak broadening (due to exchange) and side products are observed.”^[42]

Based on this observation, we can estimate the acidity of such a solution, that is, its pH value, absolute acidity, and H_0 value, to evaluate the boundary values of acidity under which the *t*Bu⁺ cation is stable.

Neat HSO_3F has a H_0 value of -15.1 . Considering an autoprotolysis constant of 10^{-7} , this value corresponds to a pH value of 3.5. In other words, an indicator base system Ind/IndH⁺ in HSO_3F that is half protonated at a H_0 value of -15.1 would have a $\text{p}K_{\text{a}}(\text{IndH}^+)$ value of 3.5. This result can be used to derive a relationship between the pH and H_0 values in HSO_3F . Thus, we obtain Equation (14) and, with the assumption that the activity coefficient of the neutral base is 1 and is unaffected by changes in concentration, we obtain Equation (15).

$$H_0 = -15.1 + \log \frac{[\text{Ind}]}{[\text{IndH}^+]} \quad (14)$$

$$\text{pH} = 3.5 + \log \frac{a(\text{Ind})}{a(\text{IndH}^+)} = 3.5 + \log \frac{[\text{Ind}]}{[\text{IndH}^+]} - \log f_{\pm} \quad (15)$$

The ion activity coefficient (f_{\pm}) can be calculated from the ion strength by using Debye–Hückel theory. From both equations, we obtain a relationship between pH and H_0 (Equation (16)).

$$H_0 = -18.6 + \text{pH} + \log f_{\pm} \quad (16)$$

No concentrations of added alcohol were reported by Olah et al.; thus, we used a concentration of 0.1 mol L^{-1} *t*BuOH as a basis for our model calculations. Considering the fact that two equivalents of HSO_3F are consumed per alcohol molecule (the formed water molecule is also protonated), we assumed an ion strength of 0.2 mol L^{-1} . With a relative dielectric constant of 120,^[43] the Debye–Hückel limiting law gave a f_{\pm} value of 0.76. From the autoprotolysis equilibrium ($\text{p}K_{\text{ap}} = 7.0$), we obtained the pH value according to Equation (17).

$$\text{pH} = 7 + \log a(\text{SO}_3\text{F}^-) = 7 + \log \frac{[\text{SO}_3\text{F}^-]}{1 \text{ mol L}^{-1}} + \log f_{\pm} \quad (17)$$

$$= 7 + \log(0.2) + \log(0.76) = 6.2$$

Inserting this value into Equation (16) gives a H_0 value according to Equation (18).

$$H_0 = -18.6 + 6.2 + \log(0.76) = -12.6 \quad (18)$$

Recently, we calculated the absolute chemical standard potential (=Gibbs standard solvation energy) of the proton in HSO_3F (i.e., at pH 0) to be -924 kJ mol^{-1} . The absolute

acidity and the absolute pH value of HSO_3F with pH 6.2 are calculated according to Equations (19) and (20).

$$\begin{aligned} \mu_{\text{abs}}(\text{H}^+) &= \Delta_{\text{soln}}G^\circ(\text{H}^+) - (RT \ln 10) \times \text{pH} \\ &= -924 \text{kJmol}^{-1} - 5.71 \text{kJmol}^{-1} \times 6.2 = -959 \text{kJmol}^{-1} \end{aligned} \quad (19)$$

$$\text{pH}_{\text{abs}} = -\frac{\mu_{\text{abs}}(\text{H}^+)}{RT \ln 10} = \frac{959 \text{kJmol}^{-1}}{5.71 \text{kJmol}^{-1}} = 168.0 \quad (20)$$

This result allows us to bracket the stability of the dissolved $\text{C}(\text{CH}_3)_3^+$ ion between H_0 values of -12.0 (in pure H_2SO_4) and -12.6 (in HSO_3F solution, see above). Within the error bars of our calculations, the absolute acidities of a 0.1M solution of the *t*Bu cation prepared from *t*BuOH in HSO_3F ($\text{pH}_{\text{abs}}=168$) and that of our RT-IL $[\text{C}(\text{CH}_3)_3]^+[\text{Al}_2\text{Br}_7]^-$ ($\text{pH}_{\text{abs}}=171$) are very similar.

Conclusion

In summary, we have shown that this simplest tertiary carbocation salt can be easily synthesised and handled at room temperature. Therefore, it can be used as a readily available source of the highly Brønsted acidic *tert*-butyl cation. Thus, we assume that this acidic IL, which is readily available in a straightforward manner and in large quantities, represents an interesting starting material or reaction medium for further reactions and investigations.

On the basis of our recently established absolute Brønsted acidity scale,^[20,21] the medium acidity of bulk $[\text{C}(\text{CH}_3)_3]^+[\text{Al}_2\text{Br}_7]^-$ and a 0.1M solution of the *t*Bu cation that was prepared from *t*BuOH in HSO_3F were almost identical. This investigation allowed us to make the first quantitative comparison between the acidities of an acidic molecular medium and an acidic ionic liquid medium. With this high acidity, the RT-IL $[\text{C}(\text{CH}_3)_3]^+[\text{Al}_2\text{Br}_7]^-$ qualifies as a cationic Brønsted acid that is on the edge of superacidity.

Experimental Section

Techniques and instruments: All of the reactions were carried out under an inert atmosphere by using standard vacuum and Schlenk techniques or in a glove box. Special Young NMR tubes and special Schlenk flasks that were sealed with Teflon or glass valves were used to exclude air and moisture. All solvents were dried over CaH_2 and distilled before use. Unlocked NMR spectroscopy was performed at RT on a Bruker Biospin Avance II 400 MHz WB spectrometer and processed with Topspin.

Synthesis and characterisation of $[\text{C}(\text{CH}_3)_3]^+[\text{Al}_2\text{Br}_7]^-$: In a typical preparation, AlBr_3 (2.00 g, 7.50 mmol) was weighed into a suitable flask inside a glove box and *tert*-butyl bromide (0.51 g, 0.42 mL, 3.75 mmol, 0.5 equiv) was condensed into it at -196°C . To stabilise the liquid, hydrogen bromide was produced in situ by adding PBr_3 (0.20 mL, 0.58 g, 2.10 mmol) to a suspension of $\text{CuSO}_4 \cdot 5\text{H}_2\text{O}$ (0.15 mg, 0.60 mmol) in toluene (5 mL). After warming the mixture at 90°C for 60 min, the HBr, which had formed by hydrolysis, was purified from the toluene and trace water by trap-to-trap condensation (-196 to -78°C) and condensed into the mixture of AlBr_3 and *tert*-butyl bromide at -78°C . Whilst stirring the mixture, it was slowly warmed to 10°C and the yellow $[\text{C}(\text{CH}_3)_3]^+$

$[\text{Al}_2\text{Br}_7]^-$ liquid was formed in 15 min in quantitative yield. The compound reversibly crystallised in a refrigerator at 2°C .

^1H NMR (104.27 MHz, 298 K): $\delta=2.6$ ppm (br s, 9H; CH_3); ^{13}C NMR (100.6 MHz, 298 K): $\delta=325$ ppm (br s, 1C; C_q), 49 (d, 9C; CH_3); ^{27}Al NMR (104.27 MHz, 298 K): $\delta=82$ ppm; IR (diamond ATR): $\tilde{\nu}=440$ (100), 696 (5), 968 (9), 1065 (15), 1283 (40), 1458 (14), 1533 (4), 2787 (37), 2953 (7), 3018 cm^{-1} (5%); FT-Raman: $\tilde{\nu}=78$ (27), 99 (37), 202 (100), 341 (4), 420 (3), 732 (1), 765 (1), 815 (2), 950 (1), 992 (1), 1089 (1), 1220 (1), 1241 (1), 1281 (4), 1295 (4), 1366 (1), 1396 (1), 1463 (1), 1488 (1), 2809 (12), 2950 (4), 2995 cm^{-1} (2%).

Crystal data for $[\text{C}(\text{CH}_3)_3]^+[\text{Al}_2\text{Br}_7]^-$: $\text{C}_4\text{H}_9\text{Al}_2\text{Br}_7$; $M_w=670.39$; monoclinic; space group $C2c$; $a=27.727(2)$, $b=13.114(1)$, $c=13.854(1)$; $\alpha=90^\circ$, $\beta=95.974(2)^\circ$, $\gamma=90^\circ$; $V=5010.0(7) \text{Å}^3$; $Z=12$; $\rho_{\text{calcd}}=2.667 \text{gcm}^{-3}$; $F(000)=3648$; $\lambda=0.71073 \text{Å}$; $T=153(2) \text{K}$; absorption coefficient = 16.889mm^{-1} ; absorption correction: multi-scan; $T_{\text{min}}=0.2852$; $T_{\text{max}}=0.7456$. Data for the structure were collected on a Bruker SMART APEX2 CCD area detector diffractometer with MoK_α radiation ($\lambda=0.71073 \text{Å}$). A single crystal was coated with perfluoroether oil at -40°C and mounted onto a 0.2mm Micromount. The structure was solved by using direct methods with SHELXTL^[44] and OLEX2^[45] and refined by least squares on weighted F^2 values for all reflections. The final refinements converged at $R_1=0.0491$ and $wR_2=0.1111$ for all reflections ($I > 2\sigma(I)$). The hydrogen atoms were included in the refinement at calculated positions by using a riding model. All attempts to locate the positions of the hydrogen atoms in the difference Fourier maps were futile.

CCDC-821960 contains the supplementary crystallographic data for this paper. These data can be obtained free of charge from The Cambridge Crystallographic Data Centre via www.ccdc.cam.ac.uk/data_request/cif.

Acknowledgements

This work was supported by the University of Freiburg, the FRIAS, the DFG, and the ERC. We also thank the Fonds der Chemischen Industrie for their support.

- [1] G. A. Olah, J. Lukas, *J. Am. Chem. Soc.* **1967**, *89*, 2227.
- [2] G. A. Olah, J. Lukas, *J. Am. Chem. Soc.* **1967**, *89*, 4739.
- [3] G. A. Olah, A. M. White, *J. Am. Chem. Soc.* **1969**, *91*, 5801.
- [4] G. A. Olah, J. S. McIntyre, I. J. Bastien, W. S. Tolgyesi, E. B. Baker, J. C. Evans, *J. Am. Chem. Soc.* **1964**, *86*, 1360.
- [5] G. A. Olah, J. S. Staral, G. Asencio, G. Liang, D. A. Forsyth, G. D. Mateescu, *J. Am. Chem. Soc.* **1978**, *100*, 6299.
- [6] S. Hollenstein, T. Laube, *J. Am. Chem. Soc.* **1993**, *115*, 7240.
- [7] P. Buzek, P. v. R Schleyer, S. Sieber, *Chem. Unserer Zeit* **1992**, *26*, 116.
- [8] T. Kato, C. A. Reed, *Angew. Chem.* **2004**, *116*, 2968; *Angew. Chem. Int. Ed.* **2004**, *43*, 2908.
- [9] M. Juhasz, S. Hoffmann, E. Stoyanov, K. C. Kim, C. A. Reed, *Angew. Chem.* **2004**, *116*, 5466; *Angew. Chem. Int. Ed.* **2004**, *43*, 5352.
- [10] E. S. Stoyanov, I. V. Stoyanova, F. S. Tham, C. A. Reed, *Angew. Chem.* **2012**, *124*, 9283; *Angew. Chem. Int. Ed.* **2012**, *51*, 9149.
- [11] T. E. Mallouk, G. L. Rosenthal, G. Muller, R. Brusasco, N. Bartlett, *Inorg. Chem.* **1984**, *23*, 3167.
- [12] L. O. Müller, D. Himmel, J. Stauffer, G. Steinfeld, J. Slattery, G. Santiso-Quinones, V. Brecht, I. Krossing, *Angew. Chem.* **2008**, *120*, 7772; *Angew. Chem. Int. Ed.* **2008**, *47*, 7659.
- [13] I. Krossing, I. Raabe, *Chem. Eur. J.* **2004**, *10*, 5017.
- [14] D. R. D. Mirda, G. M. Kramer, *J. Org. Chem.* **1979**, *44*, 2619.
- [15] F. Kalchschmid, E. Mayer, *Angew. Chem.* **1976**, *88*, 849; *Angew. Chem. Int. Ed. Engl.* **1976**, *15*, 773.
- [16] M. Ma, K. E. Johnson, *J. Am. Chem. Soc.* **1995**, *117*, 1508.
- [17] F. Kalchschmid, E. Mayer, *Z. Naturforsch. B: Chem. Sci.* **1979**, *34*, 548.

- [18] M. Blander, E. Bierwagen, K. G. Calkins, L. A. Curtiss, D. L. Price, M. L. Saboungi, *J. Chem. Phys.* **1992**, *97*, 2733.
- [19] P. Wasserscheid, T. Welton, *Ionic Liquids in Synthesis*, Wiley-VCH, Weinheim, **2008**.
- [20] D. Himmel, S. K. Goll, I. Leito, I. Krossing, *Angew. Chem.* **2010**, *122*, 7037; *Angew. Chem. Int. Ed.* **2010**, *49*, 6885.
- [21] D. Himmel, S. K. Goll, I. Leito, I. Krossing, *Chem. Eur. J.* **2011**, *17*, 5808.
- [22] G. A. Olah, D. J. Donovan, *J. Am. Chem. Soc.* **1977**, *99*, 5026.
- [23] E. Rytter, B. E. D. Rytter, H. A. Oye, J. Kroghmoe, *Acta Crystallogr. Sect. B-Struct. Sci.* **1975**, *31*, 2177.
- [24] E. Rytter, B. E. D. Rytter, H. A. Oye, J. Kroghmoe, *Acta Crystallogr. Sect. B-Struct. Sci.* **1973**, *29*, 1541.
- [25] J. J. McKinnon, D. Jayatilaka, M. A. Spackman, *Chem. Commun.* **2007**, 3814.
- [26] J. J. McKinnon, A. S. Mitchell, M. A. Spackman, *Chem. Eur. J.* **1998**, *4*, 2136.
- [27] M. A. Spackman, D. Jayatilaka, *Crystengcomm* **2009**, *11*, 19.
- [28] P. A. Wood, J. J. McKinnon, S. Parsons, E. Pidcock, M. A. Spackman, *CrystEngComm* **2008**, *10*, 368.
- [29] A. Bondi, *J. Phys. Chem.* **1964**, *68*, 441.
- [30] F. Weigend, R. Ahlrichs, *Phys. Chem. Chem. Phys.* **2005**, *7*, 3297.
- [31] S. E. Stein, in *The NIST Chemistry WebBook, NIST Standard Reference Database Number 69, Vol. 2012* (Eds.: P. J. Linstrom, W. G. Mallard), Gaithersburg MD, **2001**.
- [32] H. Feng, W. Sun, Y. Xie, H. F. Schaefer, *Chem. Eur. J.* **2011**, *17*, 10552.
- [33] G. A. Olah, G. K. S. Prakash, Á. Molnár, J. Sommer, *Superacid Chemistry*, 2nd ed., Wiley, New Jersey, **2009**.
- [34] U. Preiss, S. P. Verevkin, T. Koslowski, I. Krossing, *Chem. Eur. J.* **2011**, *17*, 6508.
- [35] U. Preiss, V. N. Emel'yanenko, S. P. Verevkin, D. Himmel, Y. U. Paulechka, I. Krossing, *ChemPhysChem* **2010**, *11*, 3425.
- [36] D. Farcasiu, S. L. Fisk, M. T. Melchior, K. D. Rose, *J. Org. Chem.* **1982**, *47*, 453.
- [37] G. M. Kramer, *J. Org. Chem.* **1975**, *40*, 298.
- [38] A. Klamt, *J. Phys. Chem.* **1995**, *99*, 2224.
- [39] A. Klamt, *COSMO-RS: From Quantum Chemistry to Fluid Phase Thermodynamics and Drug Design*, Elsevier B. V., Amsterdam, **2005**.
- [40] C. Blondel, P. Cacciani, C. Delsart, R. Trainham, *Phys. Rev. A* **1989**, *40*, 3698.
- [41] L. P. Hammett, A. J. Deyrup, *J. Am. Chem. Soc.* **1932**, *54*, 2721.
- [42] G. A. Olah, M. B. Comisarow, C. A. Cupas, C. U. Pittman, *J. Am. Chem. Soc.* **1965**, *87*, 2997.
- [43] N. J. Harris, T. Ohwada, K. Lammertsma, *J. Comput. Chem.* **1998**, *19*, 250.
- [44] G. Sheldrick, University of Göttingen, Germany.
- [45] O. V. Dolomanov, L. J. Bourhis, R. J. Gildea, J. A. K. Howard, H. Puschmann, *J. Appl. Crystallogr.* **2009**, *42*, 339.

Received: September 12, 2012
Published online: November 23, 2012